Kinetics of the gasification of a Rio Turbio coal under different pyrolysis temperatures

G. De Micco [a,b,c,*], A. Nasjleti [a], A.E. Bohé [a,b,d]

[a] Comisión Nacional de Energía Atómica (C.N.E.A.), Avenida Bustillo 9500, 8400 San Carlos de Bariloche, Argentina
[b] Consejo Nacional de Investigaciones Científicas y Técnicas (CONICET), Argentina
[c] Universidad Nacional de Cuyo, Instituto Balseiro, Avenida Bustillo 9500, 8400 San Carlos de Bariloche, Argentina
[d] Universidad Nacional del Comahue, Centro Regional Universitario Bariloche, 8400 San Carlos de Bariloche, Argentina

ARTICLE INFO

ABSTRACT

The kinetics of the gasification reaction of char with CO_2 in a fix bed reactor was studied by gas chromatography. The char was produced by devolatilizing raw coal from Rio Turbio, Argentina in a drop tube furnace (DTF). Two chars were prepared and characterized for pyrolysis temperatures of 1123 and 1223 K. The experimental conditions for chemical reaction rate control were obtained in the range of temperatures between 1098 and 1193 K. Under those conditions the influence of gasification temperature and carbon dioxide concentration was analyzed. Similar values of activation energies were obtained for both chars, and only a slight decrease in reactivity was detected for the highest pyrolyzation temperature. Regarding the effect of carbon dioxide concentrations, no influence in the gasification rate was obtained for the char pyrolyzed at 1223 K, whereas a reaction order of about 0.5 was obtained for CO_2 concentrations below 30% for the other char. Two reaction models were applied that fairly fit the experimental data: the random pore model and the grain model. The reaction rate equations according to the different models were determined.

1. Introduction

Currently, coal has a major role as an energy resource in many countries worldwide such as China, India and Australia. This is due not only because coal is an abundant, wide spread and accessible fossil fuel, but also because its mining, transportation and storage are relatively cost effectively. Even though its combustion has disadvantages from environmental point of view, because it generates greenhouse gases (CO_2) and pollutings (nitrogen and sulfur oxides), much effort is being made in the development of methods to reduce this negative effects. As an example, Integrated Gasification Combined Cycle power generation (IGCC) is one of the emerging clean coal technologies for reducing greenhouse emissions in coal-fired electricity generation [1]. The IGCC power plants provide a very high thermal efficiency, the gases produced can be used as fuel in power plants, the ash can be used as construction material or to recover valuable metals such as V and Ni. Another promising technology associated with reduction of greenhouse emissions is carbon dioxide capture and storage (CCS) which is an engineering process that involves capturing CO_2 from the electricity generation process, transporting the nearly pure CO_2 and storage of CO_2 in a storage site, usually an ocean, depleted oil or gas field or deep aquifer [2].

To design coal gasifiers, kinetic data of coal and char gasification is required. For this reason, the kinetics of the gasification reaction of different coal and chars has been studied extensively. Among these studies, the char-CO_2 gasification reaction is of great importance because it is useful to test reactivities and kinetics of different chars and coals at laboratory scale [3]. Besides, a novel method of using enriched oxygen and carbon dioxide concentrations (oxy-fuel technology) has been recently developed. This technology is based on combustion with pure oxygen instead of air, resulting in flue gas that consists mainly of CO_2 and water, that latter can be separated easily via condensation, while removing other contaminants leaving pure CO_2 for storage. However, fuel combustion in pure O_2 results in intolerably high combustion temperatures. In order to provide the dilution effect of the absent nitrogen and to moderate the furnace/combustor temperatures, part of the flue gas is recycled back into the combustion chamber [4,5].

The largest coal reservoir of Argentina is in Rio Turbio, the solid fuel available there has high potential use not only for power generation, but also for liquid fuel production from proper mixtures of H_2 and CO generated by gasification of coal. Alternatively, separating out hydrogen from the syngas it can be used as good clean fuel in hydrogen engines or fuel cells. Few studies on the reactivity and kinetics of char from Rio Turbio coal have been published [6,7], and

* Corresponding author at: Comisión Nacional de Energía Atómica (C.N.E.A.), Avenida Bustillo 9500, 8400 San Carlos de Bariloche, Argentina.
    E-mail address: demiccog@cab.cnea.gov.ar (G. De Micco).

all of them are based on thermogravimetric measurements. In this frame, this work contributes to the available gasification studies by including the effect of pyrolysis temperature in the gasification reactions. Besides, the methodology applied in this work based in gas chromatography determinations is innovative in gasification kinetic studies, since no research investigations were published using this technique with the exception of a work concerning coal steam gasification by Matsuoka et al. [8].

2. Experimental

2.1. Initial sample

The solid used in this study is an Argentinean subbituminous coal from Yacimientos Carboníferos Río Turbio (YCRT) whose composition and properties are shown in Table 1. It was ground and sieved and the particle size fraction used in this study was below 500 μm, within this range, about 60% of the particles are below 250 μm.

The char was prepared by devolatilizing the raw coal in a vertical drop tube furnace (DTF) at atmospheric pressure and two different temperatures: 1123 K (char I) and 1223 K (char II). The DTF consists of two concentric tubes of 150 cm high and 26 mm inner diameter. For the pyrolysis reaction, a nitrogen steam is preheated while it flows upwards through the annular section between the tubes, after this it enters the inner tube and the reaction takes place as it flows downwards together with the solid coal which is supplied by a feeding system with nitrogen as carrier gas. The DTF operates in laminar fluidodynamic regime, the flow of N_2 is 0.5 L/min which corresponds to a linear velocity of 1.57 cm/s. The DTF has an effective region of constant temperature of 70 cm length (corresponding to the selected pyrolysis temperature), considering that the coal particles have the same velocity of the carrier gas, the residence time in the high temperature zone is about 45 s.

During pyrolysis at 1123 K, 73% of the volatiles yield measured in the proximate analysis of the parent coal is released, while in the pyrolysis at 1223 K the amount released reaches 79% of the volatile matter yield in the proximate analysis. In Table 2 properties of chars are summarized.

Images of the coal and chars obtained with a scanning electron microscopy (SEM 515; Philips Electronics Instruments, Andover, MA) are shown in Fig. 1. Fig. 1a and b correspond to the parent

Table 1
Properties of coal.

Item	Value
Proximate analysis	
Moisture (wt%)	3.5
Volatile matter (wt%, moisture free)	37.7
Fixed carbon (wt%, moisture free)	45.2
Ash (wt%, moisture free)	17.1
Ultimate analysis (wt%, moisture free)	
Carbon	62.5
Hydrogen	5.3
Nitrogen	0.7
Sulfur	0.8
Oxygen	13.5
Ash	17.2
Other properties	
Apparent density (g/cm³)	0.67
Particle size (μm)	0–500
Elements present in ash[a]	Na, Mg, Al, Si, S, K, Ca, Ti, Fe;V, Mn
Main phases in ash[b]	Fe₂O₃, SiO₂, C (Choite), CaSO₄

[a] Energy dispersive spectroscopy (EDS) and Energy dispersive X-ray fluorescence spectroscopy (ED-XRF).
[b] X-ray diffraction (XRD).

Table 2
Properties of chars.

Item	Char I	Char II
Pyrolysis temperature (K)	1123	1223
Volatile matter (wt%, moisture free)	14	11.3
Fixed carbon (wt%, moisture free)	62.4	64.3
Ash (wt%, moisture free)	23.6	24.3
Content of (wt%, moisture free)		
Carbon	47.8	54.7
Nitrogen	0.61	1.13
Sulfur	1.4	
Apparent density (g/cm³)	0.26	0.28

coal, it can be seen that it has sharp edges, and no porosity is observed in the surface. After pyrolysis, as a consequence of gas and volatile compounds release during fast heating, an increase in surface porosity is observed, especially at the highest temperature (1223 K) Fig. 1d and f. Also a smoothness of the char particle edges can be seen in Fig. 1c and e.

2.2. Experimental setup and conditions

Gasification reactions at temperatures between 1098 and 1193 K were carried out in a tubular reactor. The gases used were CO_2 99% purity (AGA, Argentina) and Ar 99.99% purity (AGA, Argentina). The experimental setup consists in a horizontal quartz tubular reactor, a furnace, a gases control panel and a gas chromatograph SRI 8610 C with a packed column Alltech CTR I and He as carrier gas.

Solid samples of 10 mg were placed on a flat quartz crucible forming a loose packed bed, and inside the reactor where an argon flow of 3.5 L/h was maintained. For the isothermal runs, char samples were heated at the working temperature for about 1 h, after which carbon dioxide was introduced into the reactor. At the same time the exit gases were injected in a gas chromatograph every five minutes. To inject the gases in the chromatograph, the exit gases stream was connected to a 1 ml loop, and according to the gaseous flow used (4.2 L/h) the time required to load the loop was 0.86 s. The reaction rate was determined by monitoring the evolution of the reaction product concentration with time. The Reynolds number corresponding to the experimental conditions indicates that the gaseous flow inside the reactor is laminar. It has a value of 0.4 for 30% v/v of CO_2, 1193 K and 101 kPa.

2.3. Methodology

The reaction studied in this work is:

$$C(s) + CO_2(g) \rightarrow 2CO(g) \tag{1}$$

To determine the reaction kinetics, the peak areas corresponding to CO(g) concentration from the chromatograms registered every five minutes during the reactions were used. These areas are proportional to the amount of CO(g) moles formed during the time interval required to load the loop. Since this time interval (0.86 s) is very small compared with the total time necessary to achieve complete reaction (more than 3000 s), and assuming that no significant axial-mixing occurs under laminar flow condition, it can be consider that the peak areas are proportional to the instantaneous reaction rate. Plots of *CO-Area* vs. *time* were constructed for each gasification reaction, and these experimental data were fitted with appropriated curves. The number of moles formed at time *t* can be calculated by integrating the curves from 0 to *t*, and the degree of reaction at time *t* can be obtained from the ratio of the previous result and the value of integrating the whole *CO-Area* vs. *time* for the complete
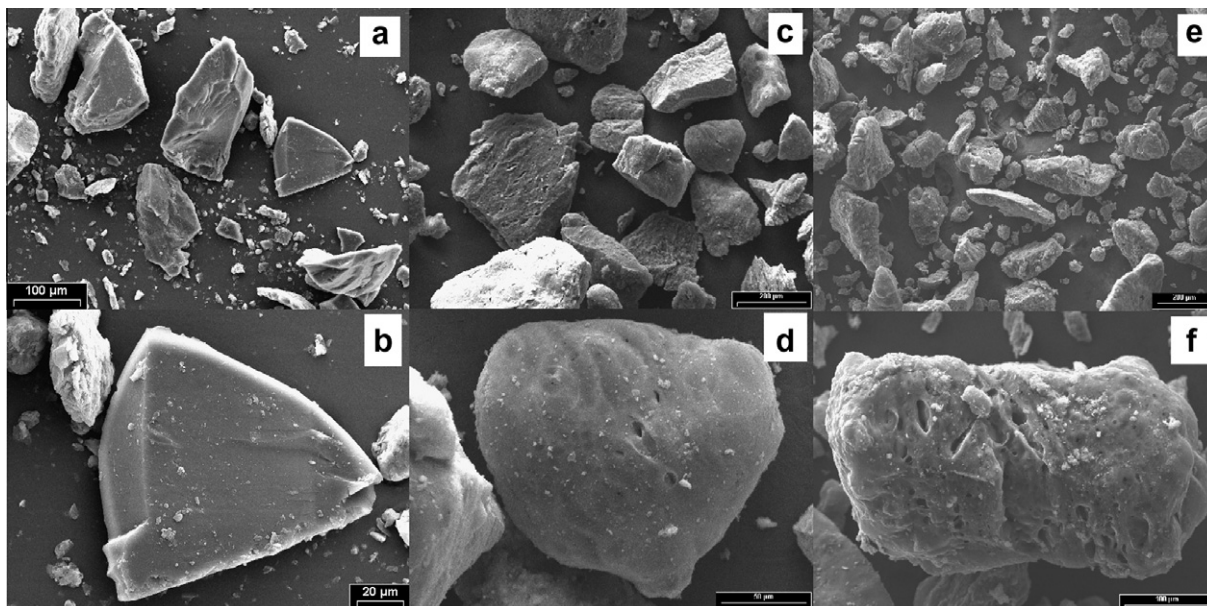
Fig. 1. SEM photographs: (a and b) parent coal, (c and d) char I (pyrolysis temperature 1123 K) (e and f) char II (pyrolysis temperature 1223 K).

gasification reaction (Eq. (2)). Plots of *degree of reaction* vs. *time* for each experiment were constructed with this procedure.

The reaction degree is defined by convenience as a function of moles of CO(g):

$$X(t) = \frac{n_{CO}(t)}{n_{CO}(t_f)} \tag{2}$$

Being $X(t)$ degree of reaction at time t, $n_{CO}(t)$ moles of CO formed from the beginning of the reaction until time t, and $n_{CO}(t_f)$ the total moles of CO(g) formed during the whole reaction.

Gasification reactions were performed at temperatures between 1098 and 1193 K. The experimental data obtained shows good reproducibility at all temperatures, the maximum variation coefficient (standard deviation/mean value) of all data series was 0.08.

3. Results and discussion

3.1. Effect of gaseous flow rate and sample mass

To find the experimental conditions under which mass-transfer resistance is absent, 30 min gasification reactions were performed at 1193 K and 30% v/v CO_2. In these experiments, the gaseous flow was increased until no changes in the reaction rate were observed and the same procedure was applied decreasing the sample mass until no change in the reaction rate was detected. The results are shown in Table 3, it can be seen that when lowering gaseous flow rate from 8.4 to 4.2 L/h for 16 mg of sample mass, no difference in the degree of reaction achieved was observed. This is indicating that the reaction is not occurring under gaseous reactant starvation condition. Additionally, calculations were made to compare the experimental rate with the rate of carbon dioxide diffusion between the top of the crucible and the top surface of the sample layer to determine whether diffusion affects the overall rate. The procedure applied for this comparison is explained in Section 4B of Ref. [9]. For all temperatures and CO_2 concentrations it was found that film diffusion is at least two orders of magnitude faster than the experimental rates indicating that gas phase diffusion had no effect in the overall rate.

Regarding the effect of sample mass, an increase in the reaction degree was achieved when sample mass was lowered from 30 to

Table 3
Influence of gaseous flow rate and sample mass in the gasification reactions.

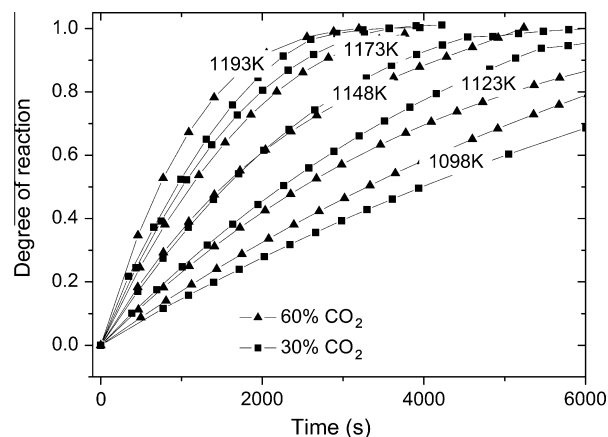| Gaseous flow rate (L/h)	Reaction degree for 30 min of gasification at 1193 K and 30% CO_2		
	Sample mass (mg)		
	10	16	30
8.4	–	0.9	–
	–	0.8	–
	–	0.8	–
4.2	0.7	1	1
	0.8	0.8	0.7
	1	0.8	0.6
	0.7	–	0.6
	0.7	–	0.6

Fig. 2. *Degree of reaction* vs. *time* curves for the gasification of char I with 30 and 60% v/v of CO_2 between 1098 and 1193 K.

16 mg. Further decrease of sample mass from 16 to 10 mg has no effect on the degree of reaction obtained. Consequently, it can be concluded that temperatures below 1193 K, gaseous flow rate of
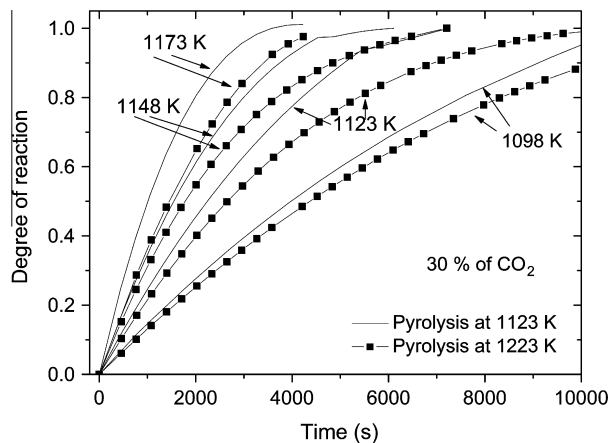
Fig. 3. *Degree of reaction* vs. *time* curves for the gasification of char I and char II with 30% v/v of CO_2 between 1098 and 1173 K.

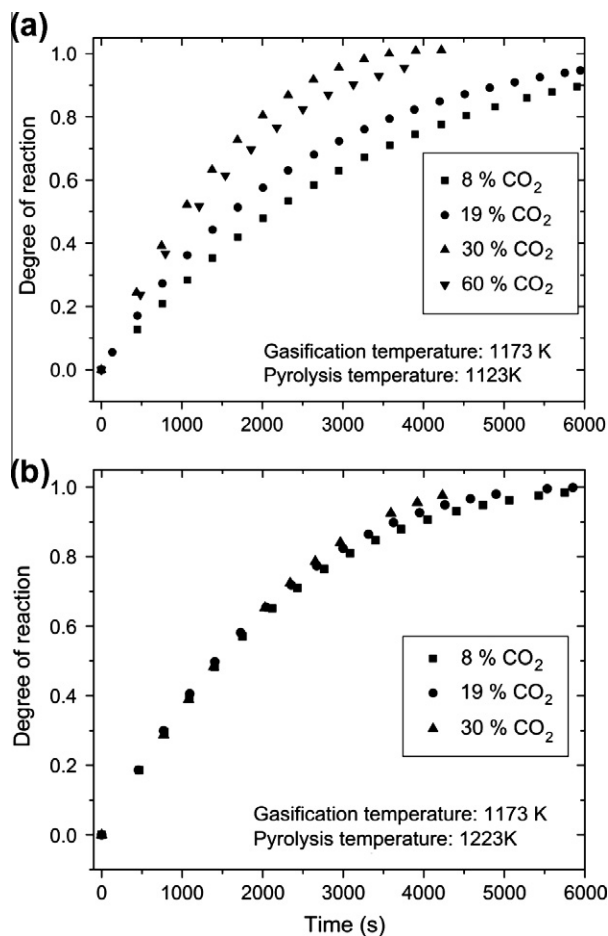**Fig. 4.** *Degree of reaction* vs. *time* curves for the gasification of char I (a) and char II (b) at 1173 K and different CO_2 concentrations.

Fig. 5. Linear fitting for the calculation of the activation energy with the free model method: (a) char I and (b) char II.

effect of diffusion in the pores within the char particles is included in the intrinsic particle kinetics because we have no control over it.

3.2. Effect of temperature and gaseous reactant concentration in gasification rate

The effect of temperature and gaseous reactant concentration in the gasification rate was analyzed for the gasification of the two chars under study. A possible kinetic expression for the reaction rate is:

$$\frac{dX}{dt} = k(T)G(C_g)f(X) \tag{3}$$

where $k(T)$ and $G(C_g)$ include the effects of temperature and gaseous reactant concentration in the reaction rate respectively, and $f(X)$ accounts for the changes in physical or chemical properties with reaction degree. The apparent reaction constant ($k(T)$) and the reactant concentration dependence $G(C_g)$ are generally assumed as:

$$k(T)G(C_g) = k_0 e^{-E_a/RT} C_g^n \tag{4}$$

the temperature dependence given by Arrhenius equation with k_0 the pre-exponential factor and E_a the activation energy, and the gas concentration dependence given by a power law expression being n the reaction order with respect to gaseous reactant concentration.

In Fig. 2 the *degree of reaction* vs. *time* curves for the gasification of char I with 30 and 60% v/v of CO_2 are shown. It can be seen that the same behavior, (i.e. an increase in the reaction rate with temperature) was obtained for both reactant concentrations, the differences in the reaction rate for 30 and 60% v/v of CO_2 at each temperature are of the same order of the experimental scattering. For this reason, it can be concluded that CO_2 concentrations higher

4.2 L/h (or higher) and sample mass of 16 mg (or lower) is enough to eliminate mass-transfer resistance.

This results are in accordance with reported behaviors for other chars in which the reaction is normally controlled by the chemical reaction and occurs nearly uniform throughout the interior surfaces of the char particles, for char particles smaller than 300 μm and temperatures below 1273 K [10–12]. However, the possible
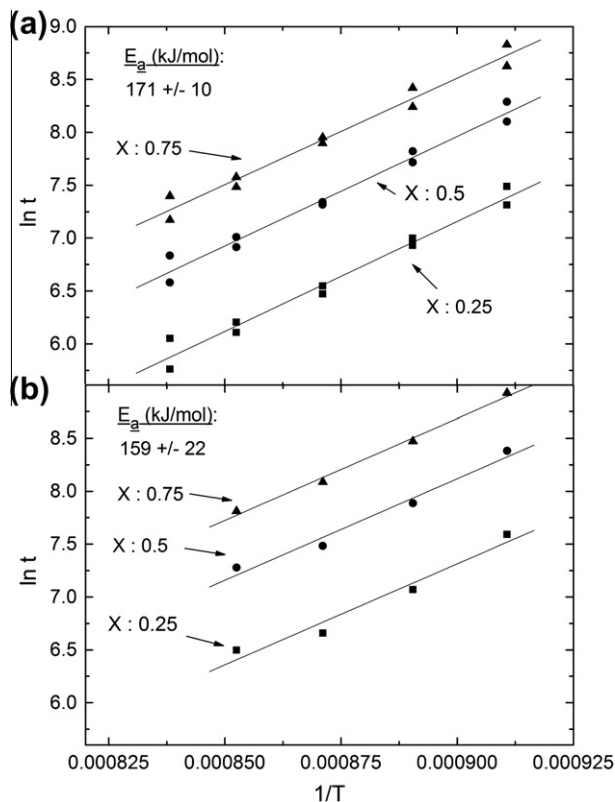
than 30% v/v have no influence in the gasification rate (i.e. the value of the reaction order n in Eq. (4) is zero).

In Fig. 3 the influence of temperature for the gasification of char II is presented. For comparison, the same curves obtained for char I are included. It can be seen that for the same temperature the reactions of char I are faster than those of char II. This behavior is indicating that there is a slight decrease in reactivity as the pyrolysis temperature increases. Several authors reported the same behavior for different gasification agents (air, steam and oxygen) for pyrolysis temperatures in the range between 973 and 1773 K [13–15]. Two plausible explanations for this behavior were proposed: firstly, the decrease in reactivity may be due to a decrease in char hydrogen content due to the increase in pyrolysis temperature. This is because part of the carbon active sites is associated with bonded hydrogen, and therefore the loss of hydrogen leads to lower reaction rates. Secondly, decreasing reactivity has been attributed to progressive thermal annealing of the chars, resulting in more ordered carbon structures, i. e., a smaller number of active surface areas [16].

The effect of gaseous reactant concentration at low concentrations of CO_2 (below 30% v/v) in the gasification of both chars was analyzed. Gasification reactions were performed at 8 and 19% v/v of CO_2. The gasification curves obtained are shown in Fig. 4. It can be seen that for the char pyrolized at 1123 K (Fig. 4a) the reaction is faster as the concentration of CO_2 increases for concentrations up to 30% v/v of CO_2. The reaction order with respect to CO_2 concentration (n in Eq. (4)) is about 0.5 in this range of concentrations. There is no consensus in the literature on the magnitude of the order of reaction and it is generally accepted that this is within the range 0.2–0.8 [3]. Ochoa et al. obtained similar reaction orders (0.5 and 0.57) for the CO_2-gasification of chars from the same precedence (Rio Turbio, Argentina) 250 μm of maximum particle diameter, prepared by pyrolyzation in a fixed reactor at 1273 K, and a 1 h treatment in nitrogen stream. The gasification conditions were 50–70% v/v of CO_2 and temperatures between 1173 and 1433 K [6].

On the other hand, for the char pyrolyzed at 1223 K (Fig. 4b) no influence of CO_2 concentration was observed in the whole range studied.

Finally, for the gasification with 8 and 19% v/v of CO_2, no substantial difference in reactivity for the different pyrolysis temperatures was observed.

Table 4
Kinetic parameters for the gasification reaction.

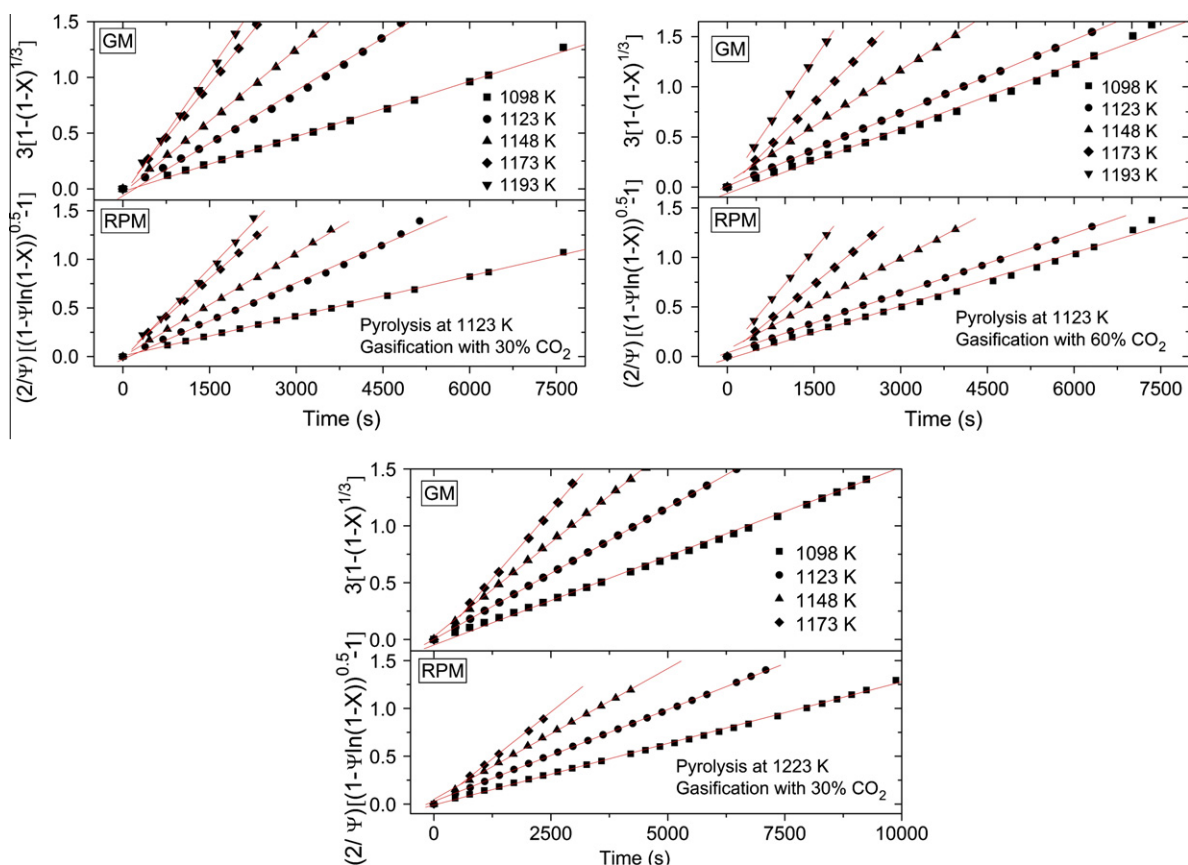| Gasification conditions	Model free method	RPM $\frac{dX}{dt} = k_0 e^{-\frac{E_a}{RT}}(1-X)\sqrt{[1-\psi \ln(1-X)]}$			GM $\frac{dX}{dt} = k_0 e^{-\frac{E_a}{RT}}(1-X)^{\frac{2}{3}}$	
	Ea (kJ/mol)	Ea (kJ/mol)	k_0 (s^{-1})	Ψ	Ea (kJ/mol)	k_0 (s^{-1})
Pyrolysis at 1123 K	171 ± 10	165 ± 11	1.15×10^4	2	166 ± 11	1.51×10^4
Pyrolysis at 1223 K	159 ± 22	158 ± 2	4.07×10^3	2	158 ± 2	5.24×10^3

Fig. 6. Linear fitting of the linearized expressions of grain model and random pore model for char I with 30 and 60% v/v of CO_2 and char II with 30% v/v of CO_2.

3.3. Kinetic parameters and reaction modeling

To determine the kinetic parameters and obtain the rate equation for the gasification reaction, two procedures were applied. Firstly, the activation energy for the gasification of char I and char II was calculated from the slope of the $\ln t$ vs $1/T$ plots (Fig. 5) according to the isoconversional method [17]. Rearranging Eq. (3):

$$\int_0^X \frac{dX}{f(X)} = \int_0^t C_g^n k_0 e^{-E_a/RT} dt \tag{5}$$

after taking integrals we have:

$$F(X) = C_g^n k_0 e^{-E_a/RT} t \tag{6}$$

By taking the logarithm of both sides of Eq. (6) one obtains:

$$\ln t = \ln\left[\frac{F(X)}{C_g^n k_0}\right] + \frac{E_a}{RT} \tag{7}$$

The first term on the right-hand side of Eq. (7) is a function of the degree of reaction and gaseous reactant concentration. Therefore, if the concentration of carbon dioxide is held constant, and the time to attain a certain reaction degree is determined as a function of temperature, Eq. (7) allows to obtain the activation energy from the slope of the plot $\ln t$ vs $1/T$, even though $f(X)$ in Eq. (3) is unknown, this procedure was applied for $X = 0.25$, 0.5 and 0.75 the values obtained are also shown in Table 4.

Secondly, the experimental degree of reaction vs. time curves were fitted with two reactions models usually applied in these kinds of gas–solid reactions: the grain model [18] and the random pore model [19]. In the grain model the surface area decreases nonlinearly with increased in reaction degree, whereas in the random pore model the reaction surface changes due to two

competing processes: the effect of pore growth during gasification and the destruction of pores due to coalescence of neighboring pores.

Replacing $f(X)$ by the GM and RPM and integrating, the linearized expressions for reaction degree vs. time are as follows:

Grain model:

$$3[1 - (1 - X)^{1/3}] = k_{GM} t \tag{8}$$

Random pore model:

$$(2/\psi)\left[\sqrt{(1 - \psi \ln(1 - X))} - 1\right] = k_{RPM} t \tag{9}$$

In the random pore model, in addition to the apparent reaction constant k_{RPM} there is another parameter, Ψ, which is related with the pore structure of the initial sample, and can be calculated from the experimental results with the following equation:

$$\psi = \frac{2}{2\ln(1 - X_{max}) + 1} \tag{10}$$

where X_{max} is the value of reaction degree where the reaction rate is maximum. In all our experiments the reaction rate is maximum
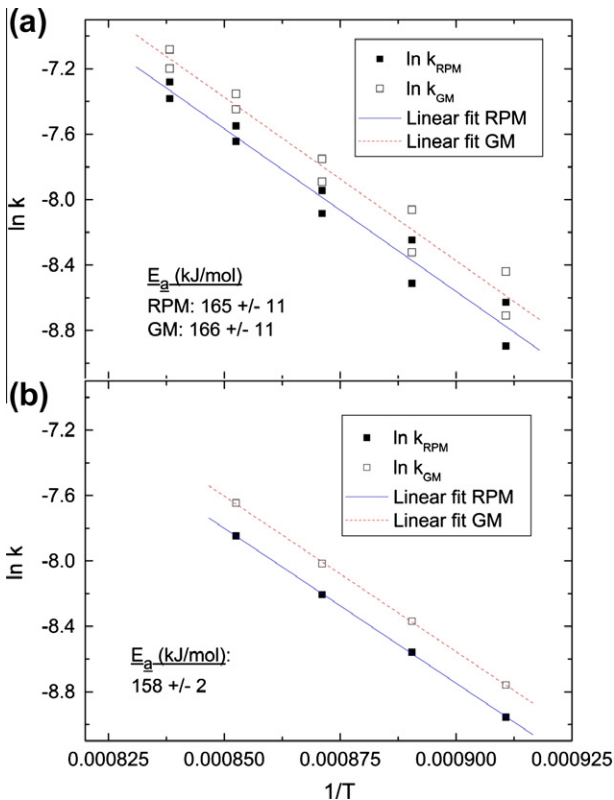

Fig. 7. Linear fitting for the calculation of the activation energy and pre-exponential factor with the random pore model and the grain model: (a) char I and (b) char II.
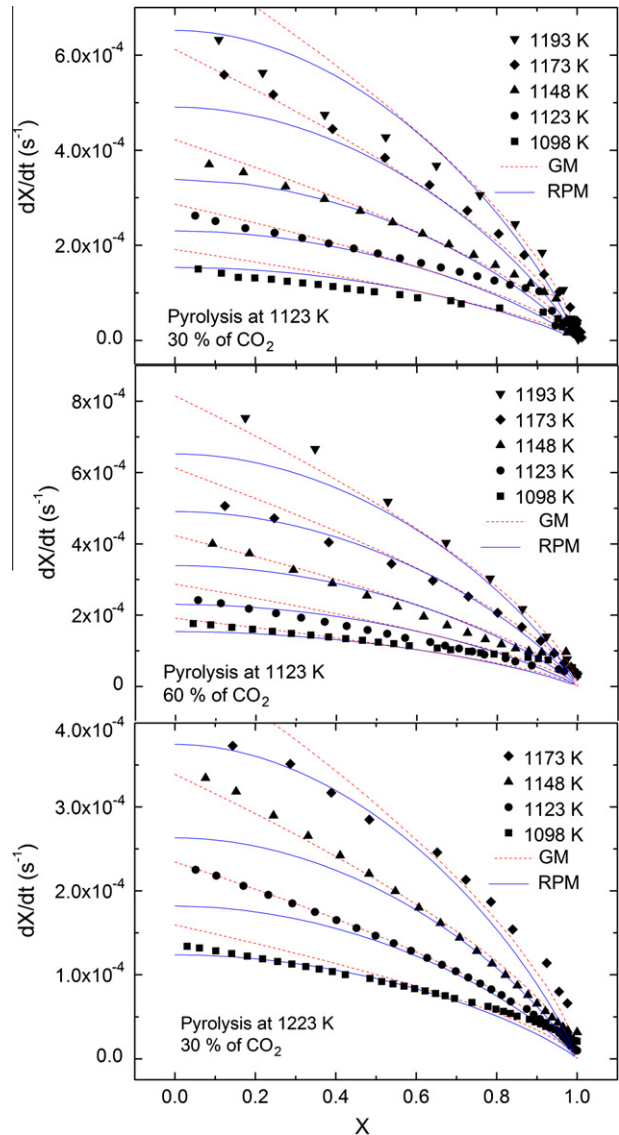

Fig. 8. Reaction rate vs reaction degree curves for the gasification of char I with 30 and 60% v/v of CO_2 and char II with 30% v/v of CO_2, and calculated reaction rate curves with random pore model and grain model.

at the beginning of the reaction ($X = 0$), consequently the value of Ψ is 2.

Fig. 6 shows that both models fit very well all the experimental data. The values of activation energy Ea and pre-exponential factor k_0 are obtained from the linear fitting of the $\ln k$ vs $1/T$ plots for each model according to Eq. (4). This is shown in Fig. 7a for char I and 7b for char II. It can be seen that the values of activation energy obtained with both models are almost the same for each char, and only a slightly lower value of Ea was obtained for the char prepared at the highest pyrolysis temperature. The activation energy values obtained are similar to those reported by Ochoa et al. [6], they obtained values of 149 and 156 kJ/mol according to random capillary model (RCM) and random pore model (RPM), for similar gasification conditions as mentioned in Section 3.2.

The kinetic parameters obtained are summarized in Table 4. Finally in Fig. 8 the *reaction rate* vs *reaction degree* curves are presented together with the calculated curves according to RPM and GM. It was found that, on average, the GM gives somewhat better description of the reaction rate than the RPM, while both models fit better the lower temperatures than the higher ones, and the higher conversion than the lower ones.

4. Conclusions

The kinetics of gasification of char from Rio Turbio coal was studied by gas chromatography. The chars were prepared by fast heating in a drop tube furnace where 73% and 79% of the volatile matter yield in the proximate analysis was released for pyrolysis temperatures of 1123 and 1223 K respectively. An increase in surface porosity of char particles was observed when increasing pyrolysis temperature. Similar values of activation energies (171 ± 10 kJ/mol for 1123 K and 159 ± 22 kJ/mol for 1223 K) were determined for both pyrolysis temperatures. Even tough the values are the same taking into account the error band, the results show that the reactivity of the chars decreases slightly with the increase in pyrolysis temperature, since the reaction rates at each temperature are systematically slower for the char produced at the highest devolatilization temperature. The activation energy values obtained in this work are lower than the activation energy obtained by us for the gasification of similar coal (191 kJ/mol [7]). However, in the previous case, the char was prepared in a tubular reactor by a 4 h treatment at 1123 K, leading to the release of all volatile matter during the pyrolysis. For the char produced at 1223 K the activation energy determined (158 kJ/mol) is the same as the value reported by Ochoa et al. [6] (156 kJ/mol) for chars prepared in a fix-bed reactor in a 1 h treatment at 1273 K. The experimental results were well correlated with two gas–solid reaction models: grain model and random pore model. Regarding the influence of CO_2 concentration, a reaction order of about 0.5 was found for the char prepared at 1123 K and only for CO_2 concentrations lower than 30% v/v. No influence in the gasification rate was observed for the char obtained at 1223 K for CO_2-concentrations between 8 and 60% v/v.

References

[1] Falcke TJ, Hoadley AFA, Brennan DJ, Sinclair SE. The sustainability of clean coal technology: IGCC with/without CCS. Process Safety Environ Prot 2011;89:41–52.
[2] Pires JCM, Martins FG, Alvim-Ferraz MCM, Simões M. Chem Eng Res Des 2011;89(9):1446–60.
[3] Muhammad FI, Muhammad U, Kusakabe K. Coal gasification in CO_2 atmosphere and its kinetics since 1948: a brief review. Energy 2011;36:12–40.
[4] Habib MA, Badr HM, Ahmed SF, Ben-Mansour R, Mezghani K, Imashuku S, et al. A review of recent developments in carbon capture utilizing oxy-fuel combustion in conventional and ion transport membrane systems. Int J Energy Res 2011;35(9):741–64.
[5] Scheffknecht G, Al-Makhadmeh1 L, Schnell U, Maier J. Oxy-fuel coal combustion—a review of the current state-of-the-art. Int J Greenhouse Gas Control 2011;5S:S16–35.
[6] Ochoa J, Casanello MC, Bonelli PR, Cukerman AL. CO_2 gasification of Argentinean coal chars: a kinetic characterization. Fuel Process Technol 2001;74:161–76.
[7] De Micco G, Fouga GG, Bohe AE. Coal gasification studies applied to H_2 production. Int J Hydrogen Energy 2010;35:6012–8.
[8] Matsuoka K, Kajiwara D, Kuramoto K, Sharma A, Suzuki Y. Factors affecting steam gasification rate of low rank coal char in a pressurized fluidized bed. Fuel Process Technol 2009;90:895–900.
[9] De Micco G, Bohé AE, Sohn HY. Intrinsic kinetics of chlorination of WO3 particles with Cl_2 gas between 973 K and 1223 K (700 °C and 950 °C). Metall Mater Trans B 2011;42(2):316–23.
[10] Sha X-Z, Chen Y-G, Cao J, Yang Y-M, Ren D-Q. Effects of operating pressure on coal gasification. Fuel 1990;69(5):656–9.
[11] Wen CY, Dutta S. In: Wen CY, Lee ES, editors. Coal conversion technology. New York: Addison-Wesley; 1979. p. 57–170 [chapter 2].
[12] Shufen L, Ruizheng S. Kinetic studies of a lingnite char pressurized gasification with CO_2, H_2, and stea. Fuel 1994;73(3):413–6.
[13] Wu S, Gu J, Li L, Wu Y, Gao J. The reactivity and kinetics of yanzhou coal chars from elevated pyrolysis temperatures during gasification in steam at 900–1200 °C. J Process Saf Environ Protect 2006;6B(84):420–8.
[14] Cai H-Y, Güell AJ, Chatzakis IN, Lim J-Y, Dugwell DR, Kandiyoti R. Combustion reactivity and morphological change in coal chars: effect of pyrolysis temperature, heating rate and pressure. Fuel 1996;75(1):15–24.
[15] Maloney DJ, Jenkins RG. Influence of coal preoxidation and the relation between char structure and gasification potential. Fuel 1985;64(10):1415–22.
[16] Fermoso J, Stevanov C, Moghtaderi B, Arias B, Pevida C, Plaza MG, et al. High-pressure gasification reactivity of biomass chars produced at different temperatures. Anal Appl Pyrol 2009;85:287–93.
[17] Friedman HL. Kinetics of thermal degradation of char-forming plastics from thermogravimetry. Application to a phenolic plastic. J Polym Sci Part C Polym Symp 1964;6(1):183–95.
[18] Szekely J, Evans JW, Sohn HY. Gas-solid reactions. New York, NY: Academic Press; 1976.
[19] Bathia SK, Perlmutter DD. A random pore model for fluid–solid reactions: I. Isothermal, kinetic control. AIChE J 1980;26(3):379–85.